Available online at www.sciencedirect.com
SCIENCE DIRECT®
Thermochimica Acta 434 (2005) 107–112
thermochimica acta
www.elsevier.com/locate/tca

Adsorption calorimetry in supported catalyst characterization: Adsorption structure sensitivity on Pt/γ-Al_2O_3

D. Uner*, M. Uner

Chemical Engineering, Middle East Technical University, Ankara 06531, Turkey

Received 8 July 2004; received in revised form 3 December 2004; accepted 25 January 2005
Available online 14 April 2005

Abstract

In this study, the structure sensitivity of hydrogen, oxygen and carbon monoxide adsorption was investigated by changing the metal particle size of Pt/Al_2O_3 catalysts. The 2% Pt/Al_2O_3 catalysts were prepared by incipient wetness method; the particle size of the catalysts was modified by calcining at different temperatures. The differential heats of adsorption of hydrogen, carbon monoxide and oxygen were measured using a SETARAM C80 Tian-Calvet calorimeter. Hydrogen chemisorption sites with low and intermediate heats were lost when the particle size increased consistent with the previous reports in the literature. No structure dependency was observed for hydrogen, carbon monoxide or oxygen initial heats of adsorption. The adsorbate:total metal stoichiometries at saturation systematically decreased with increasing particle size. While the hydrogen site energy distribution changed with increasing particle size, oxygen and carbon monoxide adsorption site energy distributions did not change appreciably with the metal particle size.

Keywords: Supported metals; Structure sensitivity; Heat of adsorption; Hydrogen; Oxygen; Carbon monoxide

1. Introduction

Many catalytic reactions are structure sensitive, the rate depends on the detailed geometrical structure of the surface atoms of the catalyst. Structure sensitivity usually manifests itself as a dependence of the rate per surface atom on the average size of the catalyst particles. The understanding is that the relative number of corner and edge sites increases dramatically with decreasing particle diameter, and these very low-coordinated surface atoms could have a substantially different ability to interact with the gas phase molecules. Norskov et al. [1] have demonstrated that the heat of adsorption of a species is directly related to the local structure of the catalysts, the step sites are more active unless poisoned, and they bind the adsorbates more strongly. The amount of heat evolved during the adsorption process, called the heat of adsorption, is closely related to the adsorbate–substrate bond strength. Furthermore, the differential heat of adsorption can be dependent on the surface coverage of the adsorbate due to the lateral adsorbate–adsorbate interactions or due to the surface heterogeneity.

The structure sensitivity of CO oxidation reaction is observed for gas phase catalytic reactions [2,3] as well as in anodic oxidation studies [4]. Both Zafiris and Gorte [2] and Gracia et al. [3] have measured lower activation energies for CO oxidation at lower dispersions. Zafiris and Gorte [2] have attributed the structure sensitivity of CO oxidation to higher desorption rates over larger particles promoted by the repulsive interactions due to the higher CO coverages on larger planes. The oxidation of CO to form CO_2 reaction proceeds via the combination of a chemisorbed CO molecule with a chemisorbed oxygen atom, the latter produced through the dissociative adsorption of O_2 on the Pt surface. Due to the poisoning effect of the CO adsorption on the Pt surface, amount of and bond strength of adsorbed oxygen on the surface gains more importance.

Structure sensitivity of CO adsorption was theoretically investigated by Hammer et al. [5]. Their predictions on well-defined crystal planes indicated strong structure sensitivity in

* Corresponding author. Tel.: +90 312 2104383; fax: +90 312 2101264.
E-mail address: uner@metu.edu.tr (D. Uner).

0040-6031/$ – see front matter © 2005 Elsevier B.V. All rights reserved.
doi:10.1016/j.tca.2005.01.058

Table 1
Literature data of CO adsorption over supported Pt surfaces

Catalyst	Percent Pt	Initial heat of adsorption (kJ/mol)	Integral heat of adsorption (kJ/mol)	Saturation coverage (μmol/g catalyst)	Dispersion (mol H ads/mol Pt)	Reference
Pt/SiO_2	1.2	144	104	48.7	1.18	[8]
$Pt–K/SiO_2$	1.2	140	101	26.7	1.31	[8]
$Pt–Sn/SiO_2$	0.93	135	83	19.6	0.51	[8]
$Pt–Sn–K//SiO_2$	0.93	138	91	10.4	0.89	[8]
Pt/SiO_2	4.0	140	105.1	130	0.51	[9]
Pt/SiO_2	7.0	140	113.8	162	0.63	[9]
Pt(2 2 1)	–	185	170	1.5 ML[a]	–	[6]
Pt(1 1 1)	–	180 ± 8	119.5	1 ML[a]	–	[10]

[a] ML: monolayer.

the adsorption energy from one structure to the other. The existence of the step sites has been demonstrated to enhance the adsorption of CO [5–7]. The initial and integral heats of CO adsorption reported in literature were collected in Table 1. The experimental data on powdered catalysts were collected at 323 K, while the single crystal data was reported to be measured at room temperature. The heat of adsorption data on two different orientations of Pt single crystal surfaces are different beyond experimental errors (Table 1). But, the structure dependency of CO chemisorption is difficult to elucidate from the literature data collected over supported metal catalysts (Table 1).

The limited amount of data on oxygen adsorption compiled in a previous publication [11] is quoted in Table 2 for reference. The adsorption heats strongly depend on whether the adsorption is molecular or dissociative. Once dissociated, oxygen forms strong bonds with the surface exceeding 250 kJ/mol. However, the adsorption of oxygen over metal surfaces is hampered by the low sticking coefficients on the surface. The dissociative sticking coefficient of oxygen was shown to increase exponentially with step concentration, adsorbed species at the steps are bound on the step edges, and dissociation almost exclusively takes place at the step sites ([21] and references therein). The existence of the step sites was demonstrated to enhance the adsorption and dissociation of oxygen [21,22].

NMR studies combined with heat of adsorption measurements indicated that hydrogen adsorption over mono and bimetallic Ru/SiO_2 catalysts is structure sensitive: hydrogen chemisorption is more facile over low coordination edge and corner sites [23–27]. The structure sensitivity of hydrogen adsorption was reflected in the calorimetry data in terms of loss of sites with low and intermediate heats in the presence of Ag or Cu atoms. However, initial heats of adsorption were not influenced in the presence of Ag or Cu. The initial and integral heats of adsorption data – measured in the vicinity of 323 K – presented in Table 3 for hydrogen over Pt do not change much with the particle size.

Therefore, the objective of this study was to measure oxygen, hydrogen and CO adsorption heats to elucidate the energetic component of structure sensitivity of adsorption over 2% Pt/Al_2O_3 by changing the particle size. Calcination temperature was selected as the parameter to modify the particle size in order to avoid complications that may arise due to the preparative chemistry.

2. Materials and methods

2.1. Sample preparation

All of the samples were prepared by incipient wetness impregnation of Pt from a solution of tetraammine platinum(II) chloride hydride (Johnson Matthey) on dried γ-Al_2O_3 (Johnson Matthey, 65 m^2/g BET surface area). The impregnation solution was prepared by dissolving an appropriate amount of $PtCl_2(NH_3)_4 \cdot H_2O$ salt in distilled water. Approximately 2 ml of solution per gram of support was needed to bring

Table 2
Adsorption modes, heats and coverages of oxygen adsorption over various surfaces of Pt [11]

Surface	Adsorption mode	Saturation coverage (ML)	Sticking coefficient, S_0	$E_{a,des}$ (kJ/mol)	ΔH_{ads} (kJ/mol)	Reference
Pt(1 1 1)	Dissociative		0.064		339 ± 32	[10]
Pt(1 1 0)	Dissociative	0.35	0.34		332 ± 10	[12]
Pt(1 1 1)		0.25	0.06	213.4–175.7		[13]
Pt(S)-[9(1 1 1)×(1 1 1)]		0.5	0.06	205–171.5		[14]
Pt(1 1 1)	Molecular	0.6			37 ± 2	[14]
Pt(1 1 1)	Dissociative	0.4			470 ± 10	[15]
Pt(1 1 1)		0.25	0.048 ± 0.006			[16]
Pt(1 1 1)		0.25				[17]
Pt(1 1 1)	Molecular peroxo				40.5	[18]
Polycrystalline Pt		0.75				[19]
Pt(1 1 1)	Molecular		0.12			[20]

Table 3
Literature data of hydrogen adsorption over supported Pt surfaces

Catalyst	Percent Pt	Initial heat of adsorption (kJ/mol)	Integral heat of adsorption (kJ/mol)	Saturation coverage (μmol/g catalyst)	Dispersion (mol H ads/mol Pt)	Reference
Pt/SiO_2	1.2	93	66	38.6	1.18	[8]
$Pt–K/SiO_2$	1.2	95	67	46.0	1.31	[8]
$Pt–Sn/SiO_2$	0.93	92	59	16.1	0.51	[8]
$Pt–Sn–K//SiO_2$	0.93	97	52	26.0	0.89	[8]
Pt/SiO_2	4.0	91	67	69	0.51	[9]
Pt/SiO_2	7.0	92	68	94	0.63	[9]

about incipient wetness. The slurries obtained after impregnation were dried overnight at room temperature and at 400 K for 2 h. The catalyst prepared as such was divided into four portions and each portion was calcined in air at a different temperature for 4 h. The calcination temperatures were selected as 410, 450, 500 and 600 °C.

2.2. Adsorption measurements

Adsorption measurements were conducted on a home built adsorption apparatus described in detail elsewhere [11]. The dispersion measurements were performed according to the method described by Uner et al. [28]. After collecting the total and weak hydrogen adsorption isotherms, the zero pressure values were obtained by extrapolating the data, the difference between the total and weak isotherm zero pressure values were reported as the strong hydrogen amounts. This value was used as the metal dispersions by assuming 1H:1 surface Pt stoichiometry for the strongly bound hydrogen.

2.3. Microcalorimetry

Heat of adsorption measurements were conducted on Setaram C-80 Tian-Calvet Calorimeter coupled to the multi-port high-vacuum Pyrex glass manifold. In this manifold a Pfeifer turbo molecular pump station backed by a diaphragm pump was used. The pressure was measured by a Baratron gauge (Varian CeramiCel) in the range of 10^{-4}–10 Torr. The details of the home made Pyrex sample and the reference cells for the calorimeter and the schematics of the set up are given in a previous publication [11]. One gram of pre-reduced and pre-calcined sample was loaded into the sample cell, which was then attached to one end of the tee connection and inserted into the sample port of the micro-calorimeter. The other end of the tee connection was attached to an empty sample cell inserted into the reference port of the micro-calorimeter. The reduction procedure described previously [11] was followed except the high pressure H_2 dosing temperature reduced to 543 K due to the maximum allowable temperature limit of the micro-calorimeter. After the reduction process the catalyst was degassed and evacuated for 10–14 h while the catalyst was very slowly cooled down to 303 K. Differential heats of adsorption were measured by introducing small amounts of gas into the sorption chamber. The amount adsorbed and heat evolution data were recorded up to the point where there was no heat signal detected upon incremental gas dosing to the limit of the pressure measurement (10 Torr).

3. Results and discussion

The hydrogen adsorption amounts as measured by volumetric chemisorption are presented in Table 4 as a function of calcination temperature. It can be seen from the data presented in Table 4 that the catalyst particle sizes could be modified by changing the calcination temperature as measured by the strongly adsorbed hydrogen stiochiometries. On the same table the saturation coverages of all adsorbates as measured by calorimetry are also presented for comparison.

Hydrogen heat of adsorption data was plotted against hydrogen coverage in Fig. 1. The coverages were determined as the ratio of the hydrogen adsorption amounts to the total hydrogen amounts measured from chemisorption experiments. Due to the upper limit of the Baratron gauge (10 Torr), the calorimetry data could not be collected till hydrogen

Table 4
Total, weak and strong hydrogen to platinum stoichiometries measured by volumetric chemisorption compared with the saturation coverages measured by microcalorimetry over 2% $Pt/\gamma\text{-}Al_2O_3$ calcined at different temperatures

Calcination temperature (°C)	By calorimetry			By volumetric chemisorption		
	CO saturation coverages (CO/Pt_{total})	O saturation coverages (O/Pt_{total})	H saturation coverages (H/Pt_{total})	Total hydrogen amounts (H_{total}/Pt)	Weak hydrogen amounts (H_{weak}/Pt)	Strong hydrogen amounts (H_{strong}/Pt)
410	0.20	0.15	>0.7	0.83	0.20	0.63
450	0.25	0.15	>0.4	0.47	0.18	0.29
500	0.10	0.12	0.20	0.26	0.06	0.20
600	0.04	0.06	0.08	0.09	0.05	0.04

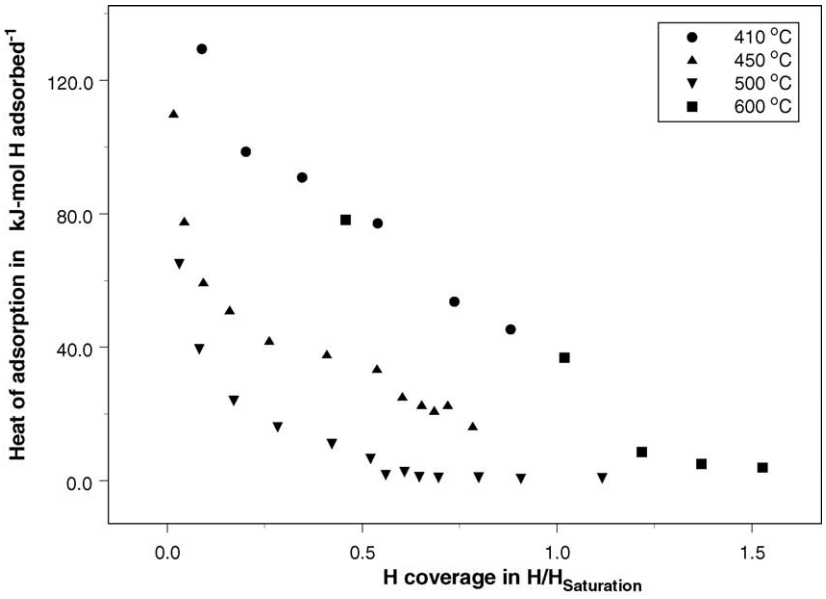

Fig. 1. Differential heat of hydrogen adsorption over 2% Pt//γ-Al_2O_3. The temperatures indicate the calcination temperature of the catalysts.

saturation – indicated by a lack of heat evolution – during the calorimetry experiments for all of the catalysts. Therefore, the coverage normalization was based on the total hydrogen amounts measured via chemisorption. The heat of adsorption data was evaluated as per mole of atomic hydrogen adsorbed. The structure sensitivity of hydrogen adsorption is evident from the data presented in Fig. 1. As observed by Narayan and King [23] and Savargaonkar et al. [24] over bimetallic catalysts, our catalysts have lost hydrogen adsorption sites with low and intermediate energies as the particle size increased, for the catalysts calcined at 450 and 500 °C. For the catalyst calcined at 600 °C, due to the low number of surface sites available for chemisorption, the sites with high initial heats could not be sampled. Furthermore, the heat of adsorption data of hydrogen over the catalyst calcined at 600 °C fell on the same curve as the data of the catalyst calcined at 410 °C. This anomaly was interpreted to be due to the high fraction of planar surfaces available on the surface of this catalyst. Because, the heats of adsorption of hydrogen values measured over these surfaces resemble the region assigned for planar surfaces in this and in previous studies [11,23,24].

Oxygen adsorption data was also plotted in terms of dissociated oxygen coverages and heats per mole of atomic oxygen (Fig. 2). The coverages were based on the saturation coverage of oxygen over the catalyst as measured by calorimetry.

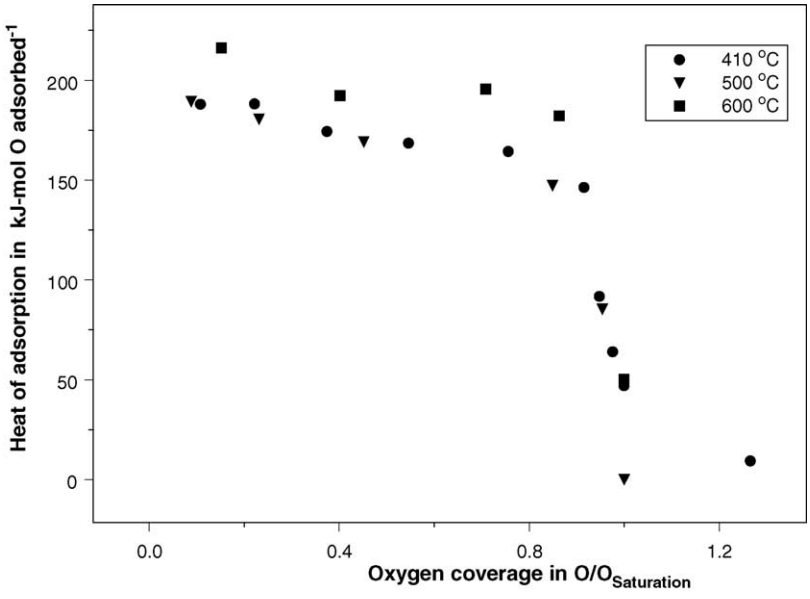

Fig. 2. Differential heat of oxygen adsorption over 2% Pt//γ-Al_2O_3. The temperatures indicate the calcination temperature of the catalysts.

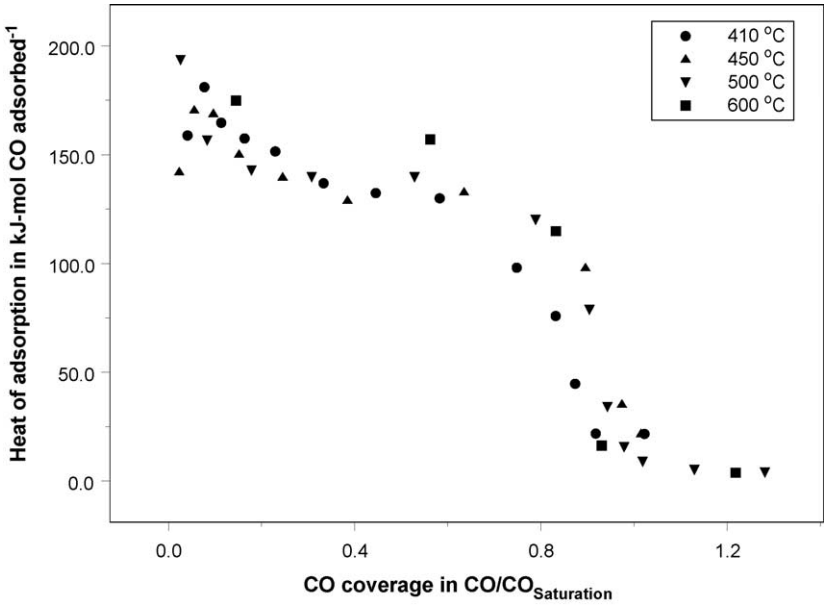

Fig. 3. Differential heat of carbon monoxide adsorption over 2% Pt//γ-Al_2O_3. The temperatures indicate the calcination temperature of the catalysts.

It is important to note here that the differential heat of adsorption curve of oxygen over the catalyst calcined at 600 °C lied systematically above the differential heat of adsorption curve of the other catalysts. This can be interpreted as a particle size effect, higher oxygen adsorption heats over larger Pt particles were measured over Pt/TiO_2 catalysts [11]. CO adsorption heats shown in Fig. 3 were also plotted against the fractional coverage determined in a similar fashion, the coverage values were normalized to the CO_{ads} saturation values as measured by calorimetry. Carbon monoxide adsorption heats do not exhibit any structure sensitivity; the heat of adsorption data for all catalysts fell on the same curve. The initial heats of adsorption and adsorption heats at saturation agree well with the literature data (Table 1) as well as the isosteric heats of adsorption measured by Dulaurent and Bianchi [29].

The number of moles of gas adsorbed at saturation per gram catalyst is plotted against the calcination temperature in Fig. 4. The decrease in the adsorbed gas amounts is consistent with the decrease in metal dispersions (Table 4). The data in Fig. 4 has some general characteristic trends. First of all, adsorbed oxygen amounts are consistently lower than that of carbon monoxide and hydrogen. Second, the decrease in adsorbed oxygen amounts with dispersion is not

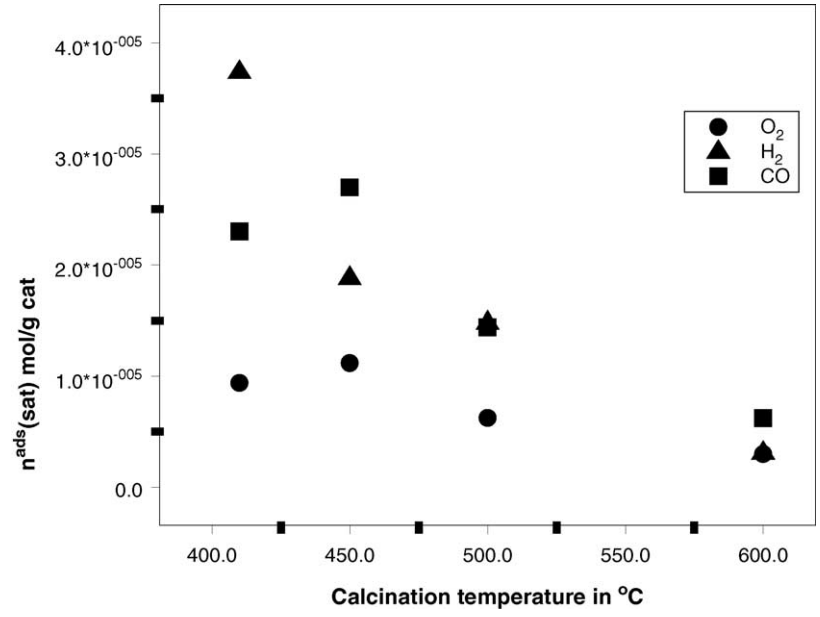

Fig. 4. The amount of gas adsorbed at saturation as a function of catalyst calcination temperature.

as pronounced as observed in hydrogen or carbon monoxide. Finally, on the catalyst calcined at 600 °C, the amount of hydrogen, oxygen and CO adsorbed approaches to similar values. Adsorbed hydrogen amounts are about twice as much as adsorbed CO or even larger for adsorbed oxygen amounts. This is believed to be due to a weakly bound hydrogen that exists on the metal surfaces at H:M stoichiometries greater than 1 [23].

From the data presented so far, one can deduce that neither initial nor integral heats of adsorption show a trend with changing metal particle size. Finally, in order to demonstrate the relative change in the adsorbent-adsorbate relationships with the metal particle size, data in Figs. 1–3 can be re-examined from the viewpoint of the adsorbate: First of all, one can easily deduce that hydrogen adsorption sites have a broader site energy distribution, the intermediate and low adsorption sites are not observed for carbon monoxide and oxygen. The broader site energy distribution monitored by hydrogen chemisorption can be attributed to the higher surface mobility of hydrogen. Carbon monoxide and oxygen adsorption energetics follow similar trends, which are not influenced by the metal particle size, while hydrogen adsorption site energy distribution is significantly altered by the particle size. The uniformity of carbon monoxide and oxygen site energy distributions can be attributed to low mobility of these adsorbates on the surface [30,31]. On the other hand, over the catalyst calcined at 600 °C, CO and O heat of adsorption curves follow similar trends, energetically and for the coverages at which they saturate the surface, while hydrogen adsorption heats exhibit a drastic decrease from high initial heats of adsorption to a very low heats of adsorption, indicating that sites with intermediate heats are completely lost upon calcination.

4. Conclusions

The structure sensitivity of hydrogen, oxygen and carbon monoxide was studied by adsorption calorimetry. The structure sensitivity of hydrogen chemisorption was observed consistent with the previous studies. The site energy distributions measured by adsorption calorimetry indicated that as the particle size decreased the site density of intermediate heats for hydrogen chemisorption decreased. On the other hand, the changes in the metal particle size did not induce a systematic change in the initial and integral heats of adsorption of CO and oxygen. CO and oxygen adsorption isotherms and heat of adsorption data resembled each other closely indicating that these molecules compete for the same kind of sites.

Acknowledgements

The financial support for this project is provided by TUBITAK under research contract no MISAG 188. The acquisition of the adsorption calorimeter was possible through a State Planning Organization Technology Research Grant no: AFP-03-04-DPT-98K122550.

References

[1] J.K. Norskov, T. Bligaard, A. Logadottir, S. Bahn, L.B. Hansen, M. Bollinger, H. Bengaard, B. Hammer, Z. Slivancanin, M. Mavrikakis, Y. Xu, S. Dahl, C.J.H. Jakobsen, J. Catal. 209 (2002) 275–278.
[2] G.S. Zafiris, R.J. Gorte, J. Catal. 140 (1993) 418–423.
[3] F.J. Gracia, L. Bollmann, E.E. Wolf, J.T. Miller, A.J. Kropf, J. Catal. 220 (2003) 382–391.
[4] W. Akemann, K.A. Friedrich, U. Linke, U. Stimming, Surf. Sci. 402–404 (1998) 571–575.
[5] B. Hammer, O.H. Nielsen, J.K. Norskov, Catal. Lett. 46 (1997) 31–35.
[6] A.D. Karmazyn, V. Fiorin, S.J. Jenkins, D.A. King, Surf. Sci. 538 (2003) 171–183.
[7] J.-S. McEwen, S.H. Payne, H.J. Kreuzer, M. Kinne, R. Denecke, H.-P. Steinruck, Surf. Sci. 545 (2003) 47–69.
[8] R.D. Cortright, J.A. Dumesic, J. Catal. 157 (1995) 576–583.
[9] S.B. Sharma, J.T. Miller, J.A. Dumesic, J. Catal. 148 (1994) 198–204.
[10] Y.Y. Yeo, L. Vattunoe, D.A. King, J. Chem. Phys. 106 (1997) 392–403.
[11] D. Uner, N.A. Tapan, I. Ozen, M. Uner, Appl. Catal. A: Gen. 251 (2003) 225–234.
[12] C.E. Wartnaby, A. Stuck, Y.Y. Yeo, D.A. King, J. Phys. Chem. 100 (1996) 12483–12488.
[13] C.T. Campbell, G. Ertl, H. Kuipers, J. Segner, Surf. Sci. 107 (1981) 220–236.
[14] K. Schwaha, E. Bechtold, Surf. Sci. 65 (1977) 277–286.
[15] J.L. Gland, B.A. Sexton, G.B. Fisher, Surf. Sci. 95 (1980) 587–602.
[16] D.R. Monroe, R.P. Merrill, J. Catal. 65 (1980) 461–469.
[17] C. Puglia, A. Nilsson, B. Hernnas, O. Karis, P. Bennich, N. Martensson, Surf. Sci. 342 (1995) 119–133.
[18] P.D. Nolan, B.R. Lutz, P.L. Tanaka, J.E. Davis, C.B. Mullins, J. Chem. Phys. 111 (1999) 3696–3704.
[19] Y.Y. Tong, J.J. Van der Klink, J. Phys. Condens. Mater. 7 (1995) 2447–2459.
[20] A. Cudok, H. Froitzheim, G. Hess, Surf. Sci. 307–309 (1994) 761–767.
[21] H. Wang, R.G. Tobin, D.K. Lambert, C.L. Di Maggio, G.B. Fisher, Surf. Sci. 372 (1997) 267–278.
[22] Z. Slivancanin, B. Hammer, Surf. Sci. 515 (2002) 235–244.
[23] R.L. Narayan, T.S. King, Thermochim. Acta 312 (1998) 105–114.
[24] N. Savargaonkar, R.L. Narayan, M. Pruski, D.O. Uner, T.S. King, J. Catal. 178 (1998) 26–33.
[25] N. Savargaonkar, D. Uner, M. Pruski, T.S. King, Langmuir 18 (2002) 4005–4009.
[26] D.P. VanderWiel, M. Pruski, T.S. King, J. Catal. 188 (1999) 186–202.
[27] N. Kumar, T.S. King, R.D. Vigil, Chem. Eng. Sci. 55 (2000) 4973–4979.
[28] D.O. Uner, M. Pruski, T.S. King, J. Catal. 156 (1995) 60–64.
[29] O. Dulaurent, D. Bianchi, Appl. Catal. A: Gen. 196 (2000) 271–280.
[30] J.M. Guil, A. Perez Masia, A. Ruiz Paniego, J.M. Trejo Menayo, Thermochim. Acta 312 (1998) 115–124.
[31] J.M. Guil, J.E. Herrero Garcia, A. Ruiz Paniego, J.M. Trejo Menayo, Top. Catal. 19 (2002) 313–321.